Available online at www.sciencedirect.com
ScienceDirect
International Journal of Heat and Mass Transfer 51 (2008) 2701–2710
International Journal of HEAT and MASS TRANSFER
www.elsevier.com/locate/ijhmt

Azimuthally dependent radiative transfer in a slab with variable refractive index

C.C. Chang, Chih-Yang Wu *

Department of Mechanical Engineering, National Cheng Kung University, Tainan 701, Taiwan, ROC

Received 21 September 2006; received in revised form 7 September 2007
Available online 3 December 2007

Abstract

Applying Fourier series expansion and a discrete ordinates method, we obtain accurate solutions of azimuthally dependent radiative transfer in an anisotropically scattering slab with variable refractive index and oblique irradiation. It is found that in a slab with a positive gradient of refractive index the optical distance traveled by incident rays decreases, and thus the value of transmittance increases. Besides, the increase of gradient of refractive index enhances the above effect. Influence of the optical thickness, scattering albedo and phase function of the medium, the incident angle of irradiation and the spatial variation of refractive index on the angular distribution of bidirectional reflectance is also investigated.

Keywords: Azimuthally dependent radiative transfer; Variable refractive index; Scattering; Fresnel reflection

1. Introduction

In the early 1990s, Siegel and Spuckler [1] investigated the effect of variable refractive index on radiative transfer in a semi-transparent layered medium. More recently, a number of ray-tracing techniques have been developed to solve the radiative transfer problems incorporating the variable refractive index [2–6]. Discrete ordinates method [7,8] and finite element method [9] were also applied to radiative transfer in media with various spatial variations of refractive index. While the emittance of a participating slab with variable refractive index evoked the wide interests [3,5], only a few papers [6,8] analysed the reflectance and transmittance of a participating slab with variable refractive index and azimuthally symmetrical irradiation. The apparent radiative properties of a participating slab are important in many heat transfer and remote sensing applications.

To understand the transport of solar radiation through atmosphere, the interaction of azimuthally dependent incident radiation with an absorbing and scattering medium that has a constant refractive index has been studied by a number of investigators [10–12]. However, it is well known that for gases in atmosphere the refractive index is a function of spatial position, because of spatial density variation. Besides, biological tissues are also scattering media with spatially variable refractive index [13]. Understanding light transport in tissues is essential for optical diagnosis and laser-induced thermal therapy. The results of a Monte Carlo simulation of laser beam propagation in a medium with constant refractive index were presented by Fowler and Menguc [14]. The above applications stimulate our interest in azimuthally dependent radiative transfer in a scattering slab with variable refractive index.

The directional-hemispherical reflectance and transmittance of a participating slab with constant refractive index have been investigated many decades ago by Pitts [15] as well as Busbridge and Orchard [11]. Furthermore, the directional-hemispherical and bidirectional reflectance and transmittance were calculated by Evans et al. [16].

* Corresponding author. Tel.: +886 6 2757575x62151; fax: +886 6 2352973.
E-mail address: cywu@mail.ncku.edu.tw (C.-Y. Wu).

0017-9310/$ - see front matter © 2007 Elsevier Ltd. All rights reserved.
doi:10.1016/j.ijheatmasstransfer.2007.10.004

Nomenclature

a_n	coefficient of scattering phase function
$a_n^{(m)}$	coefficient defined in Eq. (9a)
a_z	interpolation factor; see Eq. (28)
a_μ	interpolation factor; see Eq. (29)
A	coefficient of Eq. (30) or the absorptance $A = 1 - R - T$
B	coefficient of Eq. (30)
C	coefficient of Eq. (30)
D	source term
I	radiative intensity
I_r	reflected intensity at $z = 0$
I^k	kth coefficient of Fourier series expansion of the intensity
L	thickness of the slab
M	total number of discrete ordinates
n	refractive index
$\bar{n}$	normalized refractive index, $n(z)/n_0$
n'	gradient of the refractive index
$n_0 \to n_L$	linear refractive index, defined as $n(z) = n_0 + (n_L - n_0)z/L$
N	order of the phase function or number of spatial grids
$p(\varsigma)$	scattering phase function
P_n	Legendre polynomial
P_n^m	associated Legendre function
q_c	radiative flux of the collimated irradiation through a surface normal to the incident direction
R	directional-hemispherical reflectance
$s(z, \mu)$	curvilinear length of the ray; see Eq. (15)
S	source function
T	directional-hemispherical transmittance
w_m	weighting factor
z	geometrical coordinate

Greek symbols

α	coefficient; see Eq. (26)
β	extinction coefficient
γ	coefficient of the angular redistribution term; see Eq. (4)
δ	delta function
Δz	size of spatial grids
ς	directional cosine of the scattering angle; see Eq. (6)
θ	polar angle
μ	$\mu = \cos\theta$
ρ''	bidirectional reflectance of a slab
ρ_{ij}	interface reflectance for radiation incident on region j from region i
τ^0	optical thickness
ϕ	azimuthal angle
ω	scattering albedo
Ω	solid angle

Subscripts

0	top boundary
1	surroundings
b	index of discrete ordinates method
c	collimated irradiation or reduced collimated radiation part
e	index of discrete ordinates method
i	reduced irradiation
j	jth spatial grid
L	location $z = L$
m	mth discrete ordinate
s	fairly diffuse part due to scattering
t	index of discrete ordinates method
w	index of discrete ordinates method

Directional reflectance and transmittance from a finite scattering slab with normal incident radiation and non-unity constant refractive index were obtained by Hottel and co-workers [17]. Influence of constant refractive index on directional-hemispherical and bidirectional reflectance from a semi-infinite scattering medium with collimated incident radiation was investigated by Armaly and Lam [18]. Bidirectional reflectance for a scattering finite slab with non-unity constant refractive index was analysed by Roux and Smith [19]. A general problem of azimuthally dependent incident radiation, anisotropically scattering and reflecting boundaries were solved by Kumar and Felske [12]; they reported the reflectance, transmittance and azimuthally dependent distribution of intensities at the boundaries of a slab with unity refractive index. To our knowledge, no work has investigated azimuthally dependent radiative transfer in a scattering slab with variable refractive index.

Radiative transfer in an anisotropically scattering planar medium with variable refractive index and azimuthally dependent incident radiation is the subject of the present study. Due to azimuthally dependent incident radiation and anisotropical scattering, the radiative transfer considered is a problem with no azimuthal symmetry. The directional-hemispherical and the bidirectional reflectance and the transmittance of this case are presented. These apparent properties are dependent on the size and the absorption and scattering properties of the medium, the angular distribution of the incident radiation, and the spatial distribution of refractive index of the medium. Effects of the parameters on the apparent properties of planar media with various gradients of refractive index are investigated.

2. Analysis

We consider a planar, absorbing and anisotropically scattering medium with spatially varying refractive index, as shown in Fig. 1. At the top ($z=0$), the medium is bounded by a non-participating medium ($n_1=1$) and is exposed to collimated radiation impinging along the direction (θ_{c1},ϕ_{c1}). At the bottom ($z=L$), the medium is bounded by a cold, black substrate. The distribution of refractive index in the medium is linear, from the values n_0 to n_L; that is, $n(z)=n_0+(n_L-n_0)z/L$. Besides, it is assumed that the emission of the medium is negligible as compared with the incident radiation. The equation of radiative transfer in the medium can be expressed as

$$\mu\frac{\partial I(z,\mu,\phi)}{\partial z}+\gamma(z)\frac{\partial[(1-\mu^2)I(z,\mu,\phi)]}{\partial\mu}+\beta I(z,\mu,\phi)=S(z,\mu,\phi) \tag{1}$$

subject to the following boundary conditions:

$$I(z,\mu,\phi)|_{z=0}=q_c\frac{n_0^2}{n_1^2}(1-\rho_{10})\delta(\mu_0-\mu_{c0})\delta(\phi_0-\phi_{c0})+\rho_{01}I(z,-\mu,\phi)|_{z=0}\quad\text{for }\mu>0, \tag{2}$$

$$I(z,\mu,\phi)|_{z=L}=0\quad\text{for }\mu<0, \tag{3}$$

where I denotes the radiation intensity, $\mu=\cos\theta$ with θ denoting the angle between the positive z-axis and the direction of radiation intensity, ϕ the azimuthal angle, β the extinction coefficient, γ defined as

$$\gamma(z)=\frac{1}{n(z)}\frac{\mathrm{d}n(z)}{\mathrm{d}z}, \tag{4}$$

$S(z,\mu,\phi)$ the source function, q_c the total radiative heat flux of the collimated irradiation through a surface normal to the incident direction, ρ_{10} interface reflectance for radiation incident on the medium from surroundings, δ the Dirac-delta function, and the subscripts 0 and c the top boundary and the collimated irradiation, respectively, ρ_{01} interface reflectance for radiation incident on surroundings from the medium. Here

$$S(z,\mu,\phi)=\frac{\omega\beta}{4\pi}\int_{\phi'=0}^{2\pi}\int_{\mu'=-1}^{1}p(\varsigma)I(z,\mu',\phi')\,\mathrm{d}\mu'\,\mathrm{d}\phi', \tag{5}$$

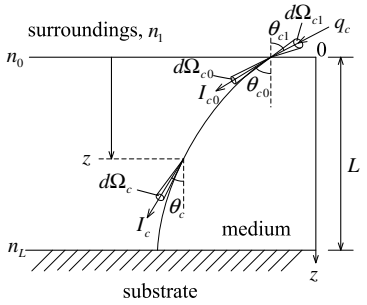

Fig. 1. Physical model and coordinate systems.

where ω is the single scattering albedo, $p(\varsigma)$ the scattering phase function and

$$\varsigma(\mu,\phi;\mu',\phi')=\mu\mu'+\sqrt{1-\mu^2}\sqrt{1-\mu'^2}\cos(\phi-\phi') \tag{6}$$

with (θ',ϕ') and (θ,ϕ) denoting the direction of the incident and scattering rays. We assume that the phase function can be expanded in terms of Legendre polynomials (P_n) in the form

$$p(\varsigma)=\sum_{n=0}^{N}a_nP_n(\varsigma),\quad a_0=1. \tag{7}$$

Here, ς is given by Eq. (6), and so the phase function can be expressed as

$$p(\varsigma)=\sum_{m=0}^{N}\sum_{n=m}^{N}(2-\delta_{0m})a_n^{(m)}P_n^m(\mu)P_n^m(\mu')\cos m(\phi-\phi'), \tag{8}$$

where

$$a_n^{(m)}\equiv a_n\frac{(n-m)!}{(n+m)!}\quad\text{for }n=m,\ldots,N\ \text{ and }\ 0\leqslant m\leqslant N, \tag{9a}$$

$$\delta_{0m}=\begin{cases}1 & \text{for } m=0,\\ 0 & \text{otherwise,}\end{cases} \tag{9b}$$

and P_n^m is the associated Legendre function.

Following Chandrasekhar [10], we divide the intensity into the reduced collimated intensity after partial extinction by absorption and out-scattering along the incident direction, I_i, and a fairly diffuse part due to the radiation scattered by the medium into the direction (θ,ϕ), I_s. With this distinction between the two parts of radiation, one can express the equation for the fairly diffuse part as

$$\mu\frac{\partial I_s(z,\mu,\phi)}{\partial z}+\gamma(z)\frac{\partial[(1-\mu^2)I_s(z,\mu,\phi)]}{\partial\mu}+\beta I_s(z,\mu,\phi)=S_i(z,\mu,\phi)+\frac{\omega\beta}{4\pi}\int_{\phi'=0}^{2\pi}\int_{\mu'=-1}^{1}p(\varsigma)I_s(z,\mu',\phi')\,\mathrm{d}\mu'\,\mathrm{d}\phi', \tag{10}$$

subject to the following boundary conditions:

$$I_s(z,\mu,\phi)|_{z=0}=\rho_{01}I_s(z,-\mu,\phi)|_{z=0}\quad\text{for }\mu>0, \tag{11}$$

$$I_s(z,\mu,\phi)|_{z=L}=0\quad\text{for }\mu<0. \tag{12}$$

Here,

$$S_i(z,\mu,\phi)=\frac{\omega\beta}{4\pi}\int_{\phi'=0}^{2\pi}\int_{\mu'=-1}^{1}p(\varsigma)I_i(z,\mu',\phi')\,\mathrm{d}\mu'\,\mathrm{d}\phi'. \tag{13}$$

The reduced collimated intensity can be expressed as

$$I_i(z,\mu,\phi)=q_c\frac{n^2(z)}{n_1^2}(1-\rho_{10})\delta(\mu_0-\mu_{c0})\delta(\phi_0-\phi_{c0})\mathrm{e}^{-\beta s(z,\mu)}, \tag{14}$$

where $s(z,\mu)$ is the curvilinear length on the ray trajectory from the top boundary to the position z. Following Ben

Abdallah and Le Dez [2], we can write the curvilinear length of the ray as

$$s(z,\mu)=\frac{\tau^0 n_0}{\beta(n_L-n_0)}\overline{n}(z)\left[\mu-\sqrt{\mu^2+\frac{1-\overline{n}^2(z)}{\overline{n}^2(z)}}\right], \tag{15}$$

where $\tau^0=\beta L$ and $\bar{n}(z)=n(z)/n_0$. Substituting Eq. (14) into Eq. (13), we obtain

$$S_i(z,\mu,\phi)=\frac{\omega\beta}{4\pi}\frac{\mu_{c1}}{\mu_c}p[\varsigma(\mu,\phi;\mu_c,\phi_c)]q_c(1-\rho_{10})\mathrm{e}^{-\beta s(z,\mu_c)}. \tag{16}$$

Here, the directional cosines at different positions on a ray are related by Snell's law. For example

$$\mu_c(z)=\sqrt{1-\frac{n_1^2(1-\mu_{c1}^2)}{n^2(z)}}. \tag{17}$$

Besides, the spatially varying refractive index has no effect on the azimuthal angle of rays, and so $\phi_c=\phi_{c0}=\phi_{c1}$.

Following Chandrasekhar [10], we expand the intensity I_s in the form:

$$I_s(z,\mu,\phi)=\sum_{k=0}^{\infty}I^k(z,\mu)\cos k(\phi_c-\phi). \tag{18}$$

Substituting Eq. (18) into Eq. (10), one can find that the resulting equation can be separated into a set of simpler equations for the functions $I^k(z,\mu)$ because of the linear independence of cos $k(\phi_c-\phi)$ [20]. By collecting the coefficient of cos $k(\phi_c-\phi)$ we obtain

$$\mu\frac{\partial I^k(z,\mu)}{\partial z}+\gamma(z)\frac{\partial[(1-\mu^2)I^k(z,\mu)]}{\partial\mu}+\beta I^k(z,\mu)=0 \quad \text{for } k>N, \tag{19}$$

$$\mu\frac{\partial I^k(z,\mu)}{\partial z}+\gamma(z)\frac{\partial[(1-\mu^2)I^k(z,\mu)]}{\partial\mu}+\beta I^k(z,\mu)=\frac{\omega\beta}{4\pi}\frac{\mu_{c1}}{\mu_c}q_c(1-\rho_{10})\mathrm{e}^{-\beta s(z,\mu)}\sum_{n=k}^{N}(2-\delta_{0k})a_n^{(k)}P_n^k(\mu)P_n^k(\mu_c)+\frac{\omega\beta}{2}\sum_{n=k}^{N}a_n^{(k)}P_n^k(\mu)\int_{\mu'=-1}^{1}P_n^k(\mu')I^k(z,\mu')\mathrm{d}\mu' \quad \text{for } k\leqslant N, \tag{20}$$

where $k=0,1,\ldots,N$ and $n=k,k+1,\ldots,N$.

Similarly, we can express the boundary conditions for these equations as

$$I^k(z,\mu)|_{z=0}=\rho_{01}I^k(z,-\mu)\quad \text{for } \mu>0, \tag{21}$$

$$I^k(z,\mu)|_{z=L}=0\quad \text{for } \mu<0. \tag{22}$$

Eq. (19) with the boundary conditions (Eqs. (21) and (22)) are all homogeneous, and so they are not needed. Therefore, the azimuthally dependent problem consisting of Eqs. (1)–(3) has been transformed into the azimuthally symmetric problem consisting of Eqs. (20)–(22).

When we consider a three-term phase function ($N=2$), we have three equations for $I^0(z,\mu)$, $I^1(z,\mu)$ and $I^2(z,\mu)$,

$$\mu\frac{\partial I^0(z,\mu)}{\partial z}+\gamma(z)\frac{\partial[(1-\mu^2)I^0(z,\mu)]}{\partial\mu}+\beta I^0(z,\mu)=\frac{\omega\beta}{4\pi}\frac{\mu_{c1}}{\mu_c}q_c(1-\rho_{10})\mathrm{e}^{-\beta s(z,\mu_c)}\times\left\{1+a_1\mu\mu_c+\frac{1}{4}a_2(3\mu^2-1)(3\mu_c^2-1)\right\}+\frac{\omega\beta}{2}\left\{\int_{\mu'=-1}^{1}I^0(z,\mu')\mathrm{d}\mu'+a_1\mu\int_{\mu'=-1}^{1}\mu' I^0(z,\mu')\mathrm{d}\mu'+\frac{1}{4}a_2(3\mu^2-1)\int_{\mu'=-1}^{1}(3\mu'^2-1)I^0(z,\mu')\,\mathrm{d}\mu'\right\}, \tag{23}$$

$$\mu\frac{\partial I^1(z,\mu)}{\partial z}+\gamma(z)\frac{\partial[(1-\mu^2)I^1(z,\mu)]}{\partial\mu}+\beta I^1(z,\mu)=\frac{\omega\beta}{4\pi}\frac{\mu_{c1}}{\mu_c}q_c(1-\rho_{10})\mathrm{e}^{-\beta s(z,\mu_c)}\times\left\{a_1\sqrt{1-\mu^2}\sqrt{1-\mu_c^2}+3a_2\sqrt{1-\mu^2}\mu\sqrt{1-\mu_c^2}\mu_c\right\}+\frac{\omega\beta}{2}\left\{\frac{1}{2}a_1\sqrt{1-\mu^2}\int_{\mu'=-1}^{1}\sqrt{1-\mu'^2}I^1(z,\mu')\mathrm{d}\mu'+\frac{3}{2}a_2\sqrt{1-\mu^2}\mu\int_{\mu'=-1}^{1}\sqrt{1-\mu'^2}\mu' I^1(z,\mu')\mathrm{d}\mu'\right\}, \tag{24}$$

$$\mu\frac{\partial I^2(z,\mu)}{\partial z}+\gamma(z)\frac{\partial[(1-\mu^2)I^2(z,\mu)]}{\partial\mu}+\beta I^2(z,\mu)=\frac{\omega\beta}{4\pi}\frac{\mu_{c1}}{\mu_c}q_c(1-\rho_{10})\mathrm{e}^{-\beta s(z,\mu_c)}\times\left\{\frac{3}{4}a_2(1-\mu^2)(1-\mu_c^2)\right\}+\frac{\omega\beta}{2}\frac{3}{8}a_2(1-\mu^2)\int_{\mu'=-1}^{1}(1-\mu'^2)I^2(z,\mu')\mathrm{d}\mu'. \tag{25}$$

All of them have the homogeneous boundary conditions, Eqs. (21) and (22). Each of the problems for the unknown functions $I^k(z,\mu)$ is similar to the radiative transfer problem solved by Lemonnier and Le Dez [7]. Here, we adapt the discrete ordinates method [7] to solve these problems. That is, we consider the function I^k along M directions with an equally spaced distribution of μ and use a constant weight quadrature, $w_m=2/M$. The function I^k is evaluated at each of the discrete directions μ_m and the angular integration in Eqs. (23), (24) or (25) is replaced by a weighted sum. Besides, the medium is divided into N slices of $\Delta z=L/N$; the unknown within the slice centers at z_j. To obtain the finite-difference of the angular redistribution term, we adopt the numerical technique proposed by Lemonnier and Le Dez [7]

$$\left\{\frac{\partial[(1-\mu^2)I_j^k]}{\partial\mu}\right\}_{\mu=\mu_m}\approx\frac{\alpha_{m+1/2}I^k_{m+1/2,j}-\alpha_{m-1/2}I^k_{m-1/2,j}}{w_m}, \tag{26}$$

where $I^k_{m\pm1/2,j}$ is the function I^k at the boundaries between two directional grids. Here, the coefficient $\alpha_{m\pm1/2}$ are given by the recursion formula

$$\alpha_{m+1/2}=\alpha_{m-1/2}-2w_m\mu_m \tag{27}$$

with $\alpha_{1/2}=0$ and $\alpha_{M+1/2}=0$.

Next, applying the spatial differencing to Eqs. (20)–(22) and integrating the resulting equations over the slice j and over the solid angle w_m around μ_m yield the discrete ordinate representation of Eqs. (20)–(22). In these equations, there are three unknown functions $(I^k_{m,e}, I^k_{t,j}, I^k_{m,j})$ while only two are known from a previous spatial step or from boundary conditions. Here, the subscripts e and t denote $e = j + \text{sign}(\mu_m)\frac{1}{2}$ and $t = m + \text{sign}(n'_j)\frac{1}{2}$, respectively. To complete the differencing procedure, we adopt the auxiliary differencing relationship developed by Lemonnier and Le Dez [7]

$$I^k_{m,e} = \frac{1}{a_z}\frac{n_e^2}{n_j^2} I^k_{m,j} + \left[1 - \frac{1}{a_z}\right]\frac{n_e^2}{n_w^2} I^k_{m,w} \quad \text{with } \frac{1}{2} \leqslant a_z \leqslant 1, \tag{28}$$

$$I^k_{t,j} = \frac{I^k_{m,j}}{a_\mu} + \left[1 - \frac{1}{a_\mu}\right] I^k_{b,j} \quad \text{with } \frac{1}{2} \leqslant a_\mu \leqslant 1, \tag{29}$$

where the subscripts w and b denote $w = j - \text{sign}(\mu_m)\frac{1}{2}$ and $b = m - \text{sign}(n'_j)\frac{1}{2}$, respectively. The above notations are developed for the convenience of sweeping the space-angle mesh. Then, we obtain the finite-difference form of Eq. (23)

$$A_m(I^k_{m,e} - I^k_{m,w}) + B_{t,j} I^k_{t,j} - B_{b,j} I^k_{b,j} + C_{m,j} I^k_{m,j} = D_{m,j} \quad \text{with } k = 0, \tag{30}$$

where $A_m = |\mu_m| w_m$, $B_{t,j} = \frac{|n^2_{j+1/2} - n^2_{j-1/2}|}{2n_j^2}\alpha_t$, $B_{b,j} = \frac{|n^2_{j+1/2} - n^2_{j-1/2}|}{2n_j^2}\alpha_b$, $C_{m,j} = \beta w_m \Delta z$, and

$$\begin{aligned} D_{m,j} = {} & w_m \Delta z \frac{\omega\beta}{4\pi} \\ & \times \left\{ \left[1 + a_1 \mu_m \mu_c(z_j) + \frac{1}{4} a_2 (3\mu_m^2 - 1)(3\mu_c^2(z_j) - 1)\right] \right. \\ & \times \frac{\mu_{c1}}{\mu_c(z_j)} q_c (1 - \rho_{10}) \mathrm{e}^{-\beta s[z_j, \mu_c(z_j)]} \\ & + 2\pi \sum_{m'=1}^{M} w_{m'} I^0_{m',j} + 2\pi a_1 \mu_m \sum_{m'=1}^{M} w_{m'} I^0_{m',j} \mu_{m'} \\ & \left. + 2\pi \frac{1}{4} a_2 (3\mu_m^2 - 1) \sum_{m'=1}^{M} w_{m'} I^0_{m',j} (3\mu_{m'}^2 - 1) \right\}. \end{aligned} \tag{31}$$

The finite-difference form of Eqs. (24) and (25) can be expressed similarly, except that the superscripts $k = 1$ and $k = 2$ for Eqs. (24) and (25), respectively, the $D_{m,j}$ corresponding to Eq. (24) is

$$\begin{aligned} D_{m,j} = {} & w_m \Delta z \frac{\omega\beta}{4\pi} \left\{ \left[a_1 \sqrt{1 - \mu_m^2}\sqrt{1 - \mu_c^2(z_j)} \right. \right. \\ & \left. + 3a_2 \sqrt{1 - \mu_m^2}\mu_m \sqrt{1 - \mu_c^2(z_j)}\mu_c(z_j) \right] \\ & \times \frac{\mu_{c1}}{\mu_c(z_j)} q_c (1 - \rho_{10}) \mathrm{e}^{-\beta s[z_j, \mu_c(z_j)]} \\ & + \pi a_1 \sqrt{1 - \mu_m^2} \sum_{m'=1}^{M} w_{m'} I^1_{m',j} \sqrt{1 - \mu_{m'}^2} \\ & \left. + 3\pi a_2 \sqrt{1 - \mu_m^2}\mu_m \sum_{m'=1}^{M} w_{m'} I^1_{j,m'} \sqrt{1 - \mu_{m'}^2}\mu_{m'} \right\} \end{aligned} \tag{32}$$

and the $D_{m,j}$ corresponding to Eq. (25) is

$$\begin{aligned} D_{m,j} = {} & w_m \Delta z \frac{\omega\beta}{4\pi} \left\{ \frac{3}{4} a_2 (1 - \mu_m^2)(1 - \mu_c^2(z_j)) \right. \\ & \times \frac{\mu_{c1}}{\mu_c(z_j)} q_c (1 - \rho_{10}) \mathrm{e}^{-\beta s[z_j, \mu_c(z_j)]} \\ & \left. + \frac{3}{4}\pi a_2 (1 - \mu_m^2) \sum_{m'=1}^{M} w_{m'} I^2_{j,m'} (1 - \mu_{m'}^2) \right\}. \end{aligned} \tag{33}$$

The boundary conditions can be expressed readily as

$$I^k_{m,1/2} = \rho_{01} I^k_{M+1-m,1/2} \quad \text{for } M/2 + 1 \leqslant m \leqslant M, \tag{34}$$

$$I^k_{m,N+1/2} = 0 \quad \text{for } 1 \leqslant m \leqslant M/2. \tag{35}$$

Eq. (30) with Eq. (31), (32) or (33) is similar to the finite-difference form of discrete ordinates equation solved by Lemonnier and Le Dez [7], except the following three points. First, the source term $D_{m,j}$ involves the unknown function $I^k_{m,j}$, and so the simultaneous solution of the system of equations has to be obtained by iteration. Second, the value of the unknown $I^1_{m,j}$ is not always positive. Thus, to solve $I^1_{m,j}$, we set the value of a_z to be unity. Third, the present results of numerical experiment have wiggles, except that we use $a_\mu = 1$. Comparisons of the results obtained by setting different values of a_μ are discussed in Section 3.

Once $I^0(z,\mu)$, $I^1(z,\mu)$ and $I^2(z,\mu)$ are known, the intensity I_s can be obtained from Eq. (18) and the intensity $I = I_s + I_i$ can be calculated. After solving I, one can obtain the radiative flux by integrating $I\mu$ over solid angle. The results in terms of dimensionless variables seem to be more general. Two of the dimensionless radiative fluxes, the directional-hemispherical reflectance and transmittance, are of practical interest. Their discrete ordinates forms are as follows:

$$R(\mu_{c1}, \phi_{c1}) = \rho_{10} + \frac{2\pi \sum_{m=1}^{M/2} w_m \mu_m (1 - \rho_{01}) I^0_{m,1/2}}{q_c \mu_{c1}}, \tag{36}$$

$$\begin{aligned} T(\mu_{c1}, \phi_{c1}) = {} & \frac{I_i(L, \mu_{cL}, \phi_c)\mu_{c1}\frac{n_0^2}{n_L^2}}{q_c \mu_{c1}} \\ & + \frac{2\pi \sum_{m=M/2+1}^{M} w_m \mu_m I^0_{m,N+1/2}}{q_c \mu_{c1}}. \end{aligned} \tag{37}$$

The energy transmitted into the substrate will eventually be absorbed, because the substrate is assumed to black. Finally, the bidirectional reflectance has the discrete ordinates form

$$\rho''(\mu_{c1}, \phi_{c1}; \mu_1, \phi_1) = \frac{I_r(0, \mu_1, \phi_1)}{q_c \mu_{c1}}, \tag{38}$$

where $I_r(0, \mu_1, \phi_1)$ is the reflected intensity and can be expressed as

$$\begin{aligned} I_r(0, \mu_1, \phi_1) = {} & \rho_{10} q_c \delta(\mu_1 + \mu_{c1}) \delta(\phi_1 - \phi_{c1} - \pi) \\ & + \frac{n_1^2}{n_0^2}(1 - \rho_{01}) I_s(0, \mu_0, \phi_0). \end{aligned} \tag{39}$$

Here μ_1 and μ_0 are related by Snell's law and $\phi_1 = \phi_0$. The first term on the right hand side of Eq. (39) is due to interface reflection, while the second term is the result of medium scattering. Besides, the bidirectional reflectance excluding interface reflection is denoted by ρ_s''. When $\mu_0 = \mu_m$

$$I_s(0,\mu_0,\phi_0) = I^0_{m,1/2} + I^1_{m,1/2}\cos(\phi_0 - \phi_c) + I^2_{m,1/2}\cos 2(\phi_0 - \phi_c). \quad (40)$$

To find the $I_s(0,\mu_0,\phi_0)$ in directions other than the direction (μ_m,ϕ_0), we can use numerical interpolation or the formal solution of radiative intensity. The formal solution can be obtained by replacing the emission term in Eq. (7) of Ref. [2] with the source function.

3. Results and discussion

Based on the preceding theoretical and numerical analyses, a computer code has been developed which is capable of modeling radiative transfer in an anisotropically scattering planar medium with variable refractive index and azimuthally dependent incident radiation. A discontinuity of refractive index at the interface results in the interface reflection and refraction, while the continuously spatial variation of the refractive index in the medium causes the curved path of the radiation streams. The present code can take both variations of refractive index into account. In a first step, we consider cases with either $n_0 = n_1$ or $n_0 \neq n_1$ to validate the code. To test the sensitivity of the method on the number of grids, N and M, the directional-hemispherical reflectance (R) and transmittance (T) of the case with $n_0 = n_1$ and $n_0 \neq n_1$ are shown in Tables 1 and 2, respectively. The latter is a case with a larger optical thickness, and so a larger number of spatial grids (N) are necessary for accurate results. Both tables show that the number of directional grids $M = 720$ is sufficiently large to generate results with four digit convergence. The number of directional grids $M = 720$ is four times of that used in azimuthally symmetrical radiative transfer [7]. Except N and M, the interpolation factor a_μ is also an important parameter of computation. Fig. 2 shows the bidirectional reflectance (ρ'') of the case with linearly anisotropic scattering, $\omega = 0.9$, $\tau^0 = 1$ and $\mu_{c1} = 0.6$. The results of the ρ'' in the plane normal to $z = 0$ surface containing the collimated irradiation ($\phi - \phi_c = 0$) are obtained by using different values of a_μ. It is readily to see the wiggles of the ρ'' curves, except those obtained by using $a_\mu = 1$. This particular choice of a_μ makes the auxiliary relationship, Eq. (29), become $I^k_{m+1/2,j} = I^k_{m,j}$ for $n'_j > 0$ and $I^k_{m-1/2,j} = I^k_{m,j}$ for $n'_j < 0$. The resulting relationship is similar to the step method applied to the slab geometry transport equation and ensures nonnegative intensity values [21]. Therefore, we use $a_\mu = 1$ in this work. The CPU time varies with computational and physical parameters described above. The number of the parameters is too large for any comprehensive coverage. However, for example, a set of R and T for the case shown in Table 1 obtained by using $N = 100$ and $M = 720$ takes 1228 seconds on a 2.66 GHz Pentium-IV personal computer. Moreover, that obtained by using $N = 200$ and $M = 720$ takes 2476 seconds and obtained by using $N = 100$ and $M = 360$ takes 305 seconds. Therefore, the CPU time seems to be approximately proportional to either N or M^2.

Since no work has investigated azimuthally dependent radiative transfer in a scattering slab with variable refrac-

Table 1
Directional-hemispherical reflectance and transmittance for the case with Rayleigh scattering, $n = 1 \to 1.5$, $\omega = 1.0$, $\tau^0 = 1.0$ and $\mu_{c1} = 0.6$

	M			
	180	360	720	1080
N = 100				
R	0.2846	0.2844	0.2843	0.2843
T	0.7154	0.7156	0.7157	0.7157
$R+T$	1.0000	1.0000	1.0000	1.0000
N = 200				
R	0.2846	0.2844	0.2843	0.2843
T	0.7154	0.7156	0.7157	0.7157
$R+T$	1.0000	1.0000	1.0000	1.0000

Table 2
Directional-hemispherical reflectance and transmittance for the case with Rayleigh scattering, $n = 1.4 \to 1.6$, $\omega = 1.0$, $\tau^0 = 5.0$ and $\mu_{c1} = 0.866$

	M			
	180	360	720	1080
N = 250				
R	0.5878	0.5876	0.5875	0.5875
T	0.4122	0.4124	0.4125	0.4125
$R+T$	1.0000	1.0000	1.0000	1.0000
N = 500				
R	0.5878	0.5876	0.5875	0.5875
T	0.4122	0.4124	0.4125	0.4125
$R+T$	1.0000	1.0000	1.0000	1.0000

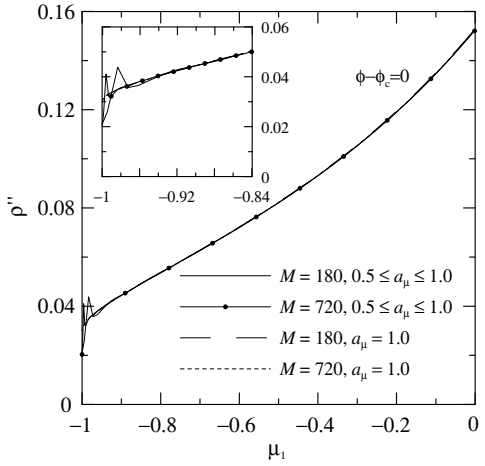

Fig. 2. Effect of a_μ on the value of $\rho''(\mu_1,\phi_c)$ for the case with $n = 1 \to 1.5$, $a_1 = 1$, $\omega = 0.9$, $\tau^0 = 1$ and $\mu_{c1} = 0.6$.

tive index, we compared our results with those obtained from the modified F_N method for cases with a unity refractive index [12]. Table 3 shows the directional-hemispherical transmittance for a weakly scattering medium with $\mu_{c1} = 0.6$ and various optical thicknesses. The normal intensities for the cases with istropical scattering and Rayleigh scattering are presented in Table 4 for a strongly scattering medium ($\omega = 0.9$). Both tables show that the present results are in excellent agreement with the results obtained from the modified F_N method.

After validating the present solution method, we investigated the effects of the parameters μ_{c1}, $n(z)$, τ^0, ω and $p(\varsigma)$ for cases with either $n_0 = n_1$ or $n_0 \neq n_1$. The latter is a bit more complicated than the former, because the latter involved both the effect of the jump of refractive index at the interface and that of the continuously spatial variation of the refractive index in the medium. To facilitate the discussion, we began with the discussion of the cases with $n_0 = n_1$. The number of parameters is too large for a comprehensive coverage. The apparent properties of planar media T, R, A (absorptance) and ρ''– are obtained for the refractive index with linear distribution, and the phase functions with $N \leqslant 2$ are considered.

Fig. 3 shows the T, R and A of a planar medium with Rayleigh scattering, $\omega = 0.9$ and $\tau^0 = 1$. From Fig. 3 the following trend may be observed. (i) As μ_{c1} decreases the optical distance traveled by the collimated irradiation increases. Thus, more energy is lost due to scattering and absorption and the value of T decreases with the decrease of μ_{c1}. (ii) When the irradiation travels from $z = 0$ to $z = L$ in a medium with a positive gradient of refractive index, the rays tend to move toward the normal. Thus, the optical distance traveled by rays decreases and the value of T increases. The larger the gradient of refractive index is, the shorter the optical distance is traveled and the larger the value of T is. (iii) By contrast, the reflectance and the absorptance decrease with the increase of gradient of refractive index.

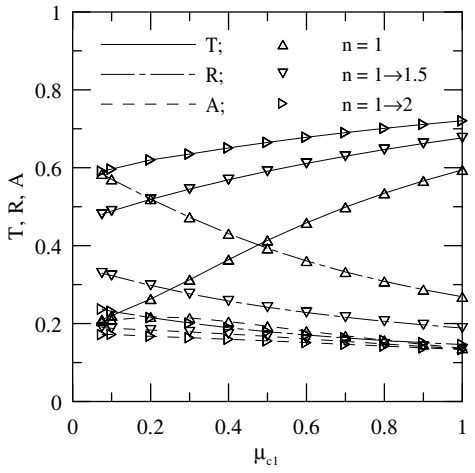

Fig. 3. Effect of angle of incidence and gradient of refractive index on the directional-hemispherical transmittance (T), reflectance (R) and absorptance (A) of the medium with Rayleigh scattering, $\omega = 0.9$, $\tau^0 = 1$ and various distributions of linear refractive index.

Comparing the lines with dots ($\tau^0 = 5$) and without dots ($\tau^0 = 1$) for a fixed value of a_1 in Fig. 4a, one may find that the value of ρ'' increases with the increase of the optical thickness. Similarly, comparing the lines with dots ($n = 1$) and without dots ($n = 1 \rightarrow 1.5$) for a fixed value of a_1 in Fig. 4b, one may find that the ρ'' decrease with the increase of gradient of refractive index. From Fig. 4 ($\theta_{c1} = 30°$) the following complicated dependence of the ρ'' on the phase function may be observed. In the plane normal to $z = 0$ surface containing the collimated irradiation, the ρ'' around the direction opposite to that of the irradiation ($\phi = \phi_c + 180°$) has a higher value for the phase function that scatters more in the backward direction ($a_1 = -1$ for the cases considered) and is lower for the more forward scattering phase function ($a_1 = 1$ for the cases considered), as shown in Fig. 4b. In the plane with $\phi = \phi_c$, the space between the curves of ρ'' for $a_1 = -1$, 0, and 1 reduces as the value of μ_1 increases. Then, each pair of the ρ'' curves intersects at a certain μ_1 and the value of ρ'' for the phase function with a small a_1 becomes less than that for the phase function with a large a_1 as the μ_1 increases further. The three curves for $a_1 = -1$, 0, and 1 intersect at more than one points, though the points of intersection are very close. The values of μ_1 at the points of intersection increase with the decrease of optical thickness or the increase of gradient of refractive index, as shown in Fig. 4.

The azimuthal distribution of reflected intensity shown in Fig. 5 reveals that radiative transfer in an anisotropically scattering medium exposed to an oblique collimated irradiation is azimuthally unsymmetrical. The reflected intensity of the nearly isotropical Rayleigh scattering is nearly azimuthally symmetrical, as shown in Fig. 5b. However, radiative transfer in an isotropically scattering medium is azimuthally symmetrical, because the source function is

Table 3
Directional-hemispherical transmittance for the case with Rayleigh scattering, $n = 1$, $\omega = 0.01$, $\mu_{c1} = 0.6$ and a variety of optical thicknesses

τ^0	T	
	Ref. [12]	This work
0.01	0.98355	0.98355
0.10	0.84712	0.84712
1.00	0.19012	0.19012
2.00	0.03618	0.03618
3.00	0.00691	0.00691
5.00	0.00026	0.00026

Table 4
Emerging intensities for the cases with $n = 1$, $\omega = 0.9$, $\mu_{c1} = 0.6$, $\tau^0 = 1.0$, isotropically scattering and Rayleigh scattering

	Isotropically scattering		Rayleigh scattering	
	Ref. [12]	This work	Ref. [12]	This work
$I(0, -1)$	0.0528	0.0528	0.0517	0.0517
$I(L,1)$	0.0450	0.0450	0.0440	0.0440

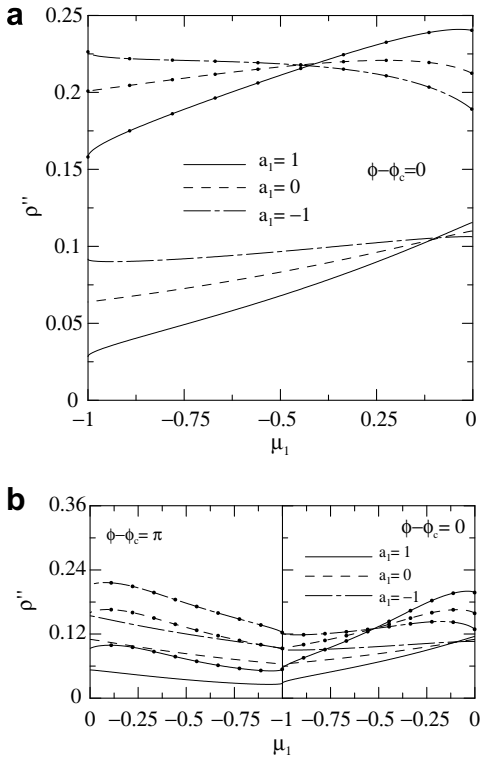

Fig. 4. Bidirectional reflectance for the cases with $\theta_{c1} = 30°$, $\omega = 1.0$ and linear phase functions: (a) effect of optical thickness $-\tau^0 = 1$ (curves without dots) and $\tau^0 = 5$ (curves with dots) for $n = 1 \rightarrow 1.5$; (b) effect of gradient of refractive index $-n = 1$ (curves with dots) and $n = 1 \rightarrow 1.5$ (curves without dots) for $\tau^0 = 1$.

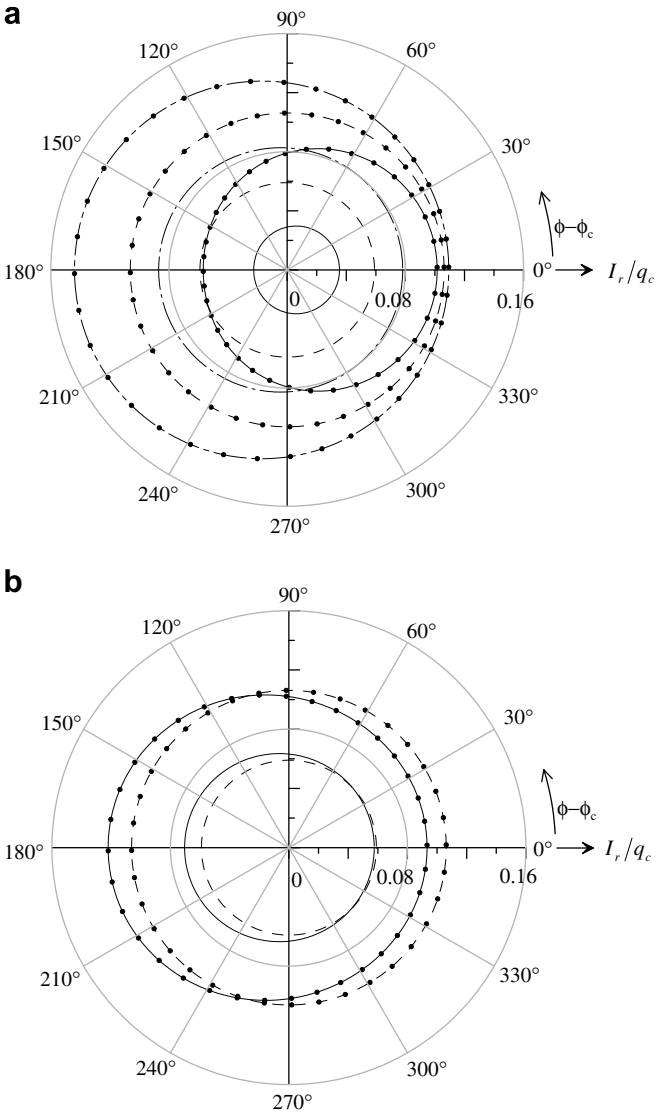

Fig. 5. Azimuthal distribution of dimensionless reflected intensity (I_r/q_c) at a fixed polar angle $\theta_1 = 150°$ for the case with $\omega = 1.0$, $\tau^0 = 1$ and $\theta_{c1} = 30°$, $n = 1$ (curves with dots) and linear refractive index $n = 1 \rightarrow 1.5$(curves without dots), and various phase functions: (a) isotropical scattering (dash curves) and linearly anisotropical scattering with $a_1 = 1$ (solid curves) and $a_1 = -1$ (alternate long and short dash curves); (b) isotropical scattering (dash curves) and Rayleigh scattering (solid curves).

still independent of direction for an isotropically scattering medium exposed to an oblique irradiation. Besides, the reflected intensity at $\phi = \phi_c$ has the highest value among the reflected intensities with the same θ_1 for the phase function that scatters most in the forward direction and, by contrast, the reflected intensity at $\phi = \phi_c + 180°$ has the highest value for the phase function that scatters most in the backward direction, as shown in Fig. 5a. Similar to the ρ'' shown in Fig. 4b, the reflected intensity of the medium with a positive gradient of refractive index is less than that of the medium with unity refractive index, as shown in Fig. 5. This is because the irradiation travels a longer optical distance in a medium with unity refractive index and so has a larger contribution of scattering to the emerging intensity at $z = 0$. Besides, it is found that the variation of refractive index does not greatly change the dependence on ϕ.

Next, the effect of the interface with $n_0 \neq n_1$ is added to the parameter investigation. The directional-hemispherical transmittance and reflectance of three media with refractive indices, $n = 1 \rightarrow 2$, $n = 1.4 \rightarrow 1.6$ and $n = 1.5$, are shown in Fig. 6. The distributions of refractive index have the same average, but different gradients. Besides, the interface at $z = 0$ of the medium with $n = 1 \rightarrow 2$ is non-reflecting, while the interface of the other two cases is reflecting. The reflectance of the interface with $n_0 \neq n_1$ is determined by Fresnel equations [20]. Fig. 6 reveals that the Fresnel reflection causes a marked decrease in the value of T and an increase in the value of R. The effect of interface reflection increases with the decrease of μ_{c1}. Comparing the curves of $n = 1.4 \rightarrow 1.6$ and $n = 1.5$, we find that the T increases and the R decreases with the increase of the gradient of refractive index. This trend is similar to that observed from the cases without interface reflection shown in Fig. 3. The effect of continuous variation of refractive index is small in comparison with that of interface reflection due to a jump of refractive index.

From Figs. 7 and 8 the following trends may be observed. (i) The value of R increases and that of T

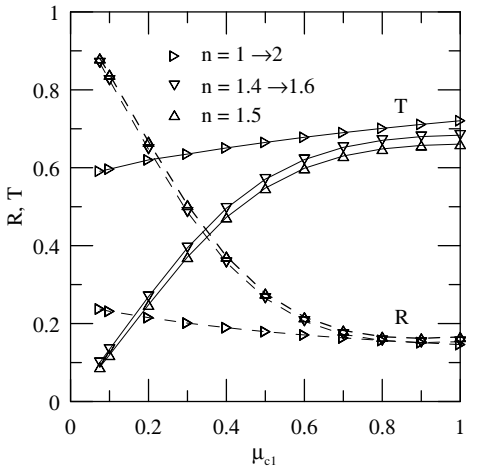

Fig. 6. Effect of angle of incidence and gradient of refractive index on the directional-hemispherical reflectance (dash curves) and transmittance (solid curves) of the medium with linear refractive index, Rayleigh scattering, $\omega = 0.9$ and $\tau^0 = 1$.

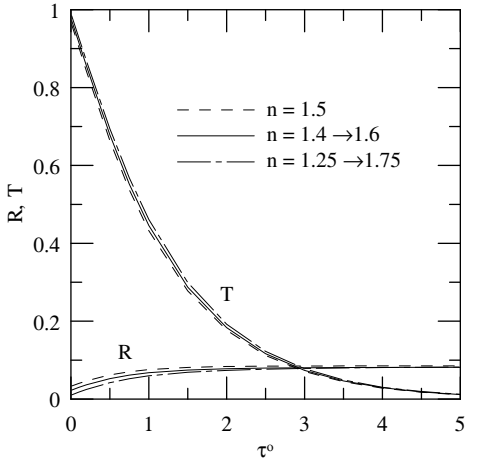

Fig. 7. Effects of optical thickness and gradient of refractive index on the directional-hemispherical reflectance and transmittance of the medium with Rayleigh scattering, $\omega = 0.5$ and $\theta_{c1} = 30°$.

decreases as the optical thickness increases. (ii) Similar to the trend observed from Fig. 6, the T increases and the R decreases with the increase of the gradient of refractive index. (iii) The spaces among the R curves and those among the T curves decrease with the decrease of the gradient of refractive index. (iv) Reducing the albedo decreases the values of R and T.

Fig. 9 shows the effects of distribution of refractive index on the bidirectional reflectance. The Fresnel reflection causes a marked variation of ρ_s'' around the glancing angle. When the gradient of refractive index is fixed, reducing the average of refractive index increases the overall magnitude of ρ_s'', as shown in Fig. 9(a). Moreover, fixing the average of refractive index and reducing the gradient of refractive index increase the overall magnitude of ρ_s'', as shown in Fig. 9b.

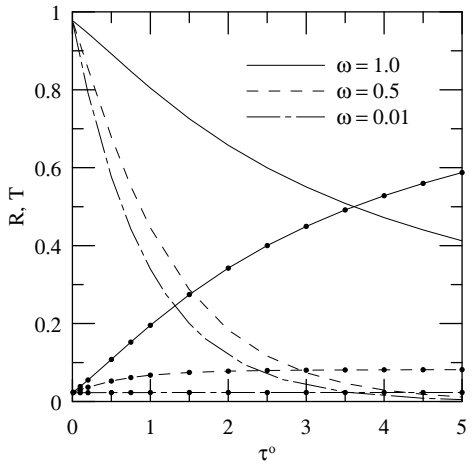

Fig. 8. Effects of albedo and optical thickness on the directional-hemispherical reflectance (curves with dots) and transmittance (curves without dots) of the medium with Rayleigh scattering, $n = 1.4 \rightarrow 1.6$ and $\theta_{c1} = 30°$.

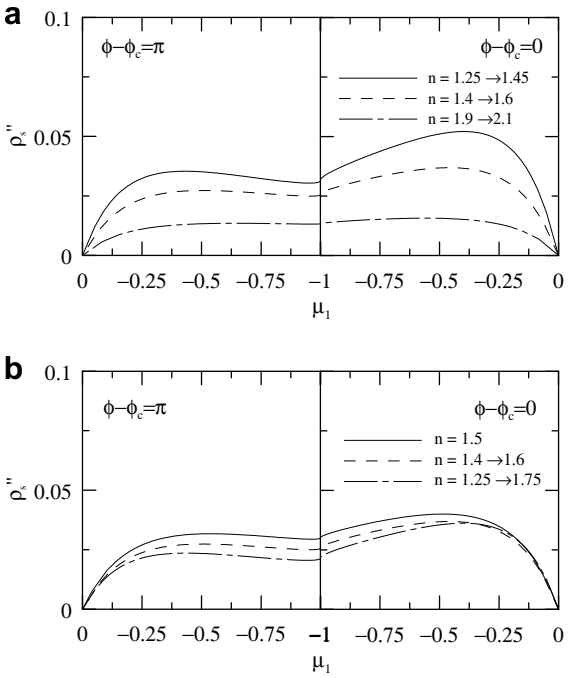

Fig. 9. Bidirectional reflectance for the cases with $a_1 = 1$, $a_2 = 0$, $\omega = 1.0$, $\tau^0 = 1$, $\theta_{c1} = 30°$ and various distributions of refractive index: (a) different averages and constant gradient of refractive index; (b) constant average and different gradients of refractive index.

4. Conclusions

This work considers azimuthally dependent radiative transfer in an anisotropically scattering slab with variable refractive index and oblique collimated irradiation. The transformation of the azimuthally dependent problem into a set of azimuthally symmetric problems follows the series expansion of the intensity proposed by Chandrasekhar [10]. Then, the discrete ordinates method has been adapted

to solve the azimuthally independent problems. After validating the present solution method, we investigate the effects of physical parameters. The following conclusions could be drawn from the apparent properties obtained:

(i) As the incident angle increases the optical distance traveled by the collimated irradiation increases, and so the magnitude of T decreases. Moreover, in a medium with a positive gradient of refractive index, the rays of the irradiation tend to move toward the normal. Thus, the optical distance traveled by incident rays decreases and the value of T increases. The increase of positive gradient of refractive index increases the magnitude of T. Reversely, the values of R and ρ'' decrease with the increase of gradient of refractive index.
(ii) The values of R and ρ'' increase as the optical thickness increases.
(iii) The value of ρ'' at $\phi = \phi_c$ has the highest value for the phase function that scatters most in the forward direction and, by contrast, the ρ'' at $\phi = \phi_c + 180°$ has the highest value for the phase function that scatters most in the backward direction.
(iv) The azimuthal distribution of reflected intensity is mainly determined by the phase function and (θ_{c1}, ϕ_{c1}). The variation of refractive index does not greatly change the dependence of ρ'' on ϕ.
(v) The effect of continuous variation of refractive index on the apparent properties is small in comparison with that of interface reflection due to a discontinuity of refractive index. The interface reflection causes a marked decrease in the value of T and an increase in the value of R.
(vi) Reducing the albedo decreases the values of R and T.
(vii) When the gradient of refractive index is fixed, reducing the average of refractive index increases the overall magnitude of ρ''_s. Besides, fixing the average of refractive index and reducing the gradient of refractive index increase the overall magnitude of ρ''_s.

References

[1] R. Siegel, C.M. Spuckler, Variable refractive index effects on radiation in semitransparent scattering multilayered regions, J. Thermophys. Heat Transfer 7 (1993) 624–630.
[2] P. Ben Abdallah, V. Le Dez, Temperature field inside an absorbing–emitting semi-transparent slab at radiative equilibrium with variable spatial refractive index, J. Quant. Spectrosc. Radiat. Transfer 65 (2000) 595–608.
[3] P. Ben Abdallah, V. Le Dez, Thermal emission of a semi-transparent slab with variable spatial refractive index, J. Quant. Spectrosc. Radiat. Transfer 67 (2000) 185–198.
[4] L.H. Liu, H.P. Tan, Q.Z. Yu, Temperature distributions in an absorbing–emitting–scattering semitransparent slab with variable spatial refractive index, Int. J. Heat Mass Transfer 46 (2003) 2917–2920.
[5] L.H. Liu, Apparent emissivity of an absorbing–emitting–scattering semitransparent slab with variable spatial refractive index, Heat Mass Transfer 40 (2004) 877–880.
[6] L.H. Liu, K. Kudo, B.X. Li, Comparison of ray-tracing methods for semitransparent slab with variable spatial refractive index, J. Quant. Spectrosc. Radiat. Transfer 85 (2004) 125–133.
[7] D. Lemonnier, V. Le Dez, Discrete ordinates solution of radiative transfer across a slab with variable refractive index, J. Quant. Spectrosc. Radiat. Transfer 73 (2002) 195–204.
[8] C.-Y. Wu, Discrete ordinates solution of transient radiative transfer in refractive planar media with pulse irradiation, in: Thirteenth International Heat Transfer Conference, Sydney, Australia, August 13–18, 2006.
[9] L.H. Liu, Finite element solution of radiative transfer across a slab with variable spatial refractive index, Int. J. Heat Mass Transfer 48 (2005) 2917–2920.
[10] S. Chandrasekhar, Radiative Transfer, Dover, New York, 1960.
[11] I.W. Busbridge, S.E. Orchard, Reflection and transmission of light by a thick atmosphere according to a phase function: $1 + x\cos\theta$, Astrophys. J. 149 (1967) 644–655.
[12] S. Kumar, J.D. Felske, Radiative transport in a planar medium exposed to azimuthally unsymmetric incident radiation, J. Quant. Spectrosc. Radiat. Transfer 35 (1986) 187–212.
[13] G.J. Tearney, M.E. Brezinski, J.F. Southern, B.E. Bouma, M.R. Hee, J.G. Fujimoto, Determination of the refractive index of highly scattering human tissue by optical coherence tomography, Opt. Lett. 20 (1995) 2258–2260.
[14] A.J. Fowler, M.P. Menguc, Propagation of focused and multibeam laser energy in biological tissue, J. Biomech. Eng. 122 (2000) 534–540.
[15] E. Pitts, The application of radiative transfer theory to scattering effects in unexposed photographic emulsions, Proc. Phys. Soc. B 67 (1954) 105–119.
[16] L.B. Evans, C.M. Chu, S.W. Churchill, The effect of anisotropic scattering on radiant transport, J. Heat Transfer 87C (1965) 381–387.
[17] H.C. Hottel, A.F. Sarofim, L.B. Evans, I.A. Vasalos, Radiative transfer in anisotropically scattering media: allowance for Fresenl reflection at the boundaries, J. Heat Transfer 90 (1968) 56–62.
[18] B.F. Armaly, T.T. Lam, Influence of refractive index on reflectance from a semi-infinite absorbing–scattering medium with collimated incident radiation, Int. J. Heat Mass Transfer 18 (1975) 893–900.
[19] J.A. Roux, A.M. Smith, Biangular reflectance for an absorbing and isotropically scattering medium, AIAA J. 23 (4) (1985) 624–628.
[20] M.N. Özisik, Radiative Transfer, John Wiley and Sons, New York, 1973.
[21] B.G. Carlson, K.D. Lathop, Transport theory – the method of discrete ordinates, in: H. Greenspan, C.N. Kelber, D. Okrent (Eds.), Computing Methods in Reactor Physics, Goldon and Breach, New York, 1968 (Chapter 3).